Since January 2020 Elsevier has created a COVID-19 resource centre with free information in English and Mandarin on the novel coronavirus COVID-19. The COVID-19 resource centre is hosted on Elsevier Connect, the company's public news and information website.

Measurement 164 (2020) 108031

Contents lists available at ScienceDirect

Measurement

journal homepage: www.elsevier.com/locate/measurement

On the wavelet-based compressibility of continuous-time sampled ECG signal for e-health applications

Asma Maalej [a], Manel Ben-Romdhane [a,*], Mariam Tlili [b], François Rivet [c], Dominique Dallet [c], Chiheb Rebai [a]

[a] COSIM Research Lab., SUP'COM, University of Carthage, Cité Technologique des Communications, 2083 El Ghazala, Ariana, Tunisia
[b] LIP6, CNRS, Sorbonne University, 4 Place Jussieu, F-75005 Paris, France
[c] IMS Laboratory, University of Bordeaux, BORDEAUX INP ENSEIRB-MATMECA, 351 Cours de la Libération, 33405 Talence, France

ARTICLE INFO

Article history:
Received 19 March 2020
Received in revised form 1 May 2020
Accepted 22 May 2020
Available online 27 May 2020

Keywords:
ECG
LC-ADC
PRD
Wavelet families
Compression
Thresholding process

ABSTRACT

This paper presents a compression study of electrocardiogram (ECG) signals for e-Health cardiac online diagnostic systems. The study uses 75 real electrocardiogram records sampled with continuous-time level-crossing (LC) analog-to-digital converter (ADC). This signal-dependent LC-ADC compresses signals compared to conventional ADC but further compression is needed especially for long-time monitoring applications. The orthogonal matching pursuit algorithm is simulated to evaluate ECG compression with 54 orthogonal and biorthogonal wavelets. For LC-ADC amplitude output compression, Biorthogonal3.1 (bior3.1) wavelet achieves optimal performances in terms of compression ratio (CR) while ensuring 2-% percentage root-mean-square difference (PRD). The PRD must be limited to this value to ensure a very good quality signals after decompression. For circuit implementation purposes, bior3.1 wavelet is proposed as a multiplier-free decomposition step and a noncomplex global and hard thresholding process is achieved. The average CR is 63% and PRD varies between 0.1 and 2.1% leading to a very good diagnostic quality.

1. Introduction

Since the discovery of the electrical activity of the heart by Einthoven in 1895 [1], electrocardiogram (ECG) monitoring has expended from basic heart rhythm detection to complex heart disease diagnosis. It has been shown that the medical information carried in the ECG is valuable to achieve early diagnosis, then to prevent or to treat cardiovascular diseases (CVDs). For the most of heart pathologies, the long-term monitoring of cardiovascular signs is needed. In such situation, a wearable and connected ECG healthcare device is required as it increases user's comfort by allowing his mobility. Wireless monitoring is also adopted in remote diagnosis systems, which are proposed as a solution to healthcare issue for low-income, hard-to-reach or rural zones [2,3]. It is recently involved in health crisis such as Coronavirus Disease 2016 (Covid-19) pandemic either to monitor patients on lockdown or to free up beds for the sickest Covid-19 patients [4].

In addition to patient monitoring, the ECG is recently involved in innovative biomedical applications such as decision support system to help in the diagnosis of ambiguous cases or as a biometric signal for authentication and identification [5,6]. The latter solutions involve the machine learning algorithms for classification and utilize intrinsically the wavelet transform as a feature extractor [2,3,5–8].

Depending on the utilization of the ECG, the acquisition of this biomedical signal differs. For example, the detection and the diagnosis of CVDs like ischemic, cryptogenic and coronary heart diseases require extensive wireless ECG monitoring over the course of months to years. In these sophisticated application, a 12-lead, portable and low-power device is required [9]. For instance, to prevent from cryptogenic strokes, monitoring using a 12-lead ECG over up to 24 h with a 12-bit analog-to-digital converter (ADC) that samples the ECG signal at a frequency of 1 kilo samples per second (kS/s), produces almost 1.5 Giga bytes [10]. Online processing of this huge amount of data requires high operational power and high memory resources [11].

Due to ECG low innovation rate feature, many compression techniques have been proposed to optimize the digitized data with a conventional ADC [12–16]. In fact, considering ECG characteristics, redundant and non-significant measurements are eliminated. Furthermore, compression algorithms are followed by encoding methods to reduce binary length of computed symbols [17]. As many works propose different solutions for signal compression like the power spectral density, proposed in [18], when the relevant

* Corresponding author.
E-mail address: manel.benromdhane@supcom.tn (M. Ben-Romdhane).

https://doi.org/10.1016/j.measurement.2020.108031
0263-2241/

information are retrieved via spectral analysis of biomedical signals, the discrete wavelet transform (DWT) still widely used to eliminate samples via a threshold while computing the sparse transform of the acquired electrocardiogram signal [12,19,20]. Hybrid decompositions and integrated circuit approaches for mobile tele-cardiology have been proposed. These approaches yield high compression ratios (CRs) and improved energy efficiency [17,19,20].

Thus far, most of the attempts and implemented solutions are interested in reducing data volumes independently from the sampling step [20,21]. This conventional acquisition paradigm suffers from three limitations [22]. First, focusing only on data compression after sampling reduces the activity of the transmission or storage modules and ignores the acquisition ones, especially analog circuits activity. Second, compression of huge amount of data often requires large buffers and many computational iterations. Third, as ECG is always digitized at a constant frequency, its low innovation rate feature is disregarded. Exhausting activity of pre- and post-compression modules is therefore inevitable.

Thus, in order to relax compression requirements and data volumes, a signal-dependent ADC architecture is interesting [23–25]. In the last decade, sampling with level-crossing ADC (LC-ADC) has caught researchers' attention. In fact, it only acquires relevant information by comparing the signal to a specific set of levels. Thus, sampling frequency changes according to signal variation and the circuit activity is reduced [23–25]. Thanks to ECG low innovation rate feature, less data is processed after sampling compared to the conventional ADC.

Certainly, the LC-ADC reduces the mean sampling rate but it delivers the samples and their quantized time intervals. Therefore, ECG compression is still needed especially with long-time monitoring. Besides, the system would benefit from higher compression ratios, lower complexity and lower power consumption than those reached by using only the LC-ADC [26]. To the best of the authors' knowledge, while many works have been interested in compression of discrete-time sampled data [12,19,20], no study to date is reported about compression of continuous-time sampled ECG with the DWT and by applying threshold [3,6,17,19,20]. Thus, in this paper, the authors propose to extend their DWT-based compression study of continuous-time sampled electrocardiogram data to achieve better CRs. As it is a common powerful tool often applied in conventional ECG signal processing, authors propose to estimate DWT compression for all available wavelets on Matlab. In fact, Matlab tools cover a very large variety of wavelet families including the ones usually used with ECG signals. The obtained results for LC-ADC output samples and time intervals lead the authors to choose the best-fit DWT case and to propose a design of the compression step based on multiplier-free wavelet transform and a noncomplex thresholding process.

The remainder of this paper is organized as follows. Section 2 presents the LC-ADC and its inherent compression performances. Section 3 develops the compression method proposed for this work including a brief description of the wavelet transform, the compression study steps and the design of the whole stage. In Section 4, comparative performance results are discussed to identify the best-fit DWT to compress the LC-ADC output samples. Design of the DWT filter bank compression and threshold application are also proposed besides of performances results. Then, Section 5 discusses compression results of the LC-ADC time intervals output. Finally, Section 6 concludes the paper and draws some future works.

2. LC-ADC for ECG sampling and compression

The level-crossing (LC) sampling has been introduced since the 80′s as a compression technique associated with digital encoding [27]. In the last decade, it has been studied with speech and biological signals [28,29]. Some circuits have been proposed for biosignal acquisitions, ranging from LC-ADCs in application-specific integrated circuits (ASICs) [23,25], to fully integrated system on chip (SoC) solutions for wearable sensors [30] and implementations with low-cost micro-controllers [31]. In this section, the authors present the LC-ADC architecture and its inherent compression performances.

2.1. LC-ADC architecture

The converter's block diagram is shown in Fig. 1 [32]. The input signal, ECG_{in}, is continuously compared to two reference levels. When a LC event is detected by the comparators, digital values of the reference levels are updated. Then, the M-bit digital-to-analog converter (DAC) produces the updated analog reference voltages. Moreover, a control logic is used to set the digital value of the crossed level, ECG_{out}, as the output sample [24]. In fact, the LC-ADC signal-dependency is due to this behavior. Thus, when the signal's amplitude is not varying, the LC-ADC is not activated, which makes it suitable for ECG sampling. In fact, when ECG signal does not vary significantly as in the interval between T and P waves, low number of samples will be digitized. To recover the signal from the continuous-time sampled data, time information is needed to localize in time the LC events. Therefore, the time-tracking stage, including an N-bit counter synchronized at a clock frequency, F_c, computes the duration, TI, between two successive LC events. An example of LC-ADC output samples versus the original signal is given in Fig. 2 where q is the quantization step obtained by dividing LC-ADC full scale by the total number of reference levels [32].

To measure LC-ADC performances, a detailed LC-ADC model was implemented in Matlab/SIMULINK and designed according to ECG signal specifications in terms of amplitude and frequency [23,25]. The next subsection presents some LC-ADC compression performances and compares them to discrete-time sampling output.

2.2. LC-ADC compression performances

For a given duration, DT, as for example 1 s, compression performances of the LC-ADC are compared to those of conventional ADC.

Comparison parameters are the mean sampling frequency, F_{mean}, and the LC-ADC compression ratio, CR_{LC-ADC}, as in (1) and (2),

$$F_{mean} = \frac{1}{N_{LC-ADC}.F_c} \sum_{i=1}^{N_{LC-ADC}} TI_i \tag{1}$$

$$CR_{LC-ADC} = \frac{mN_{ADC} - (M+N)N_{LC-ADC}}{mN_{ADC}} \tag{2}$$

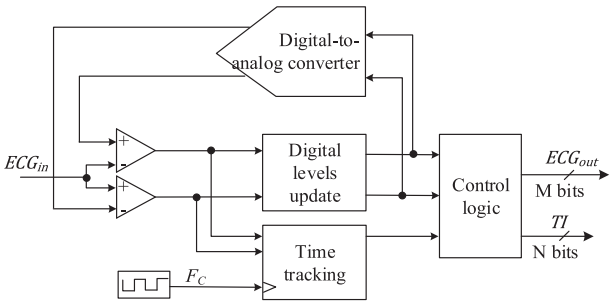

Fig. 1. Signal-dependent LC-ADC block diagram.

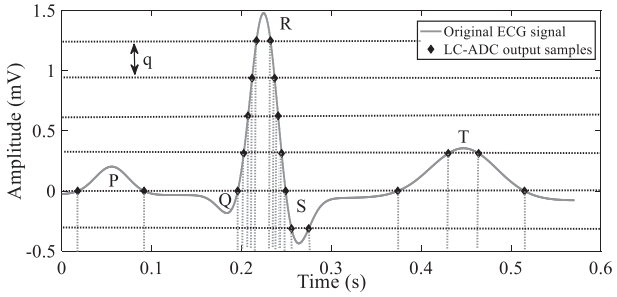

Fig. 2. Level-crossing sampling for a 3-bit LC-ADC.

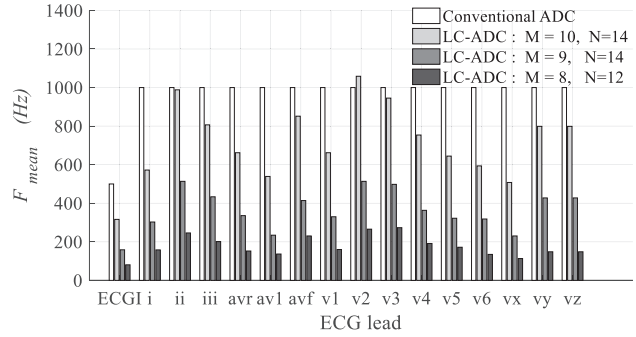

Fig. 4. Mean sampling frequency versus ECG leads, LC-ADC resolution and counter resolution.

where m is the conventional ADC resolution, M is the resolution of the LC-ADC amplitude output, ECG_{out}, N is the LC-ADC counter resolution, N_{ADC} is the number of ADC samples during DT and N_{LC-ADC} is the number of LC-ADC samples during DT.

Behavioral simulations are done with 16 real ECG records from Physionet database [33]. These signals are composed of a normal 1-lead ECG, *rec_1val*, from *ECG-ID* database, and a 15-lead ECG, *s0101lrem*, from *PTB-diagnostic* database reflecting myocardial infarction [34]. The normal ECG lead I, recorded for 20 s, is digitized at 500 samples per second with 12-bit resolution. Besides, each one of the 15 lead ECG signals is digitized at 1 kilo samples per second (kS/s) samples per second, with 16-bit resolution. Firstly, the signals are up-sampled at 1-MHz frequency. This step is done to obtain a pseudo analog form of the signal comparing to the sampling frequency applied in Nyquist [24,35]. Secondly, since the LC-ADC resolution, M, has an impact on the quantization step, the converter's model is simulated with M varying from 8 to 10 bits [24]. These values are typical for ECG amplitude quantization and also ensure good quality reconstructed signals which require at least 8-bit resolution [11,24,32,36]. The LC-ADC full scale was set to 10 mV. As far as the counter resolution is concerned, N, it is equal to 12 bits for an 8-bit LC-ADC and 14 bits for 9- and 10-bit LC-ADCs [32]. Simulations have been carried out over one period of every ECG lead which contains a P wave followed by a QRS complex then a T wave as presented in Fig. 2.

The CR_{LC-ADC} and the F_{mean} performances are given in Fig. 3 and Fig. 4, respectively, where *ECGI* is the normal I-lead record, and the other leads are the 15 leads of a myocardial infarction record. As shown in Fig. 3, an 8-bit LC-ADC and a 9-bit LC-ADC achieve CR_{LC-ADC} as computed regarding (2) up to 81% and 55.8%, respectively. However, for a 10-bit resolution, no compression is realized at all, resulting in a 0-% CR_{LC-ADC}.

For performances regarding the mean sampling frequency of the LC-ADC, the original sampling frequency, as indicated in Physionet database, is depicted in Fig. 4. Mean sampling frequency of the LC-ADC, as computed regarding (1), is at least 50% and 75% lower than for the conventional ADC uniform sampling in the case of 9-bit and 8-bit resolution, respectively. As expected, the mean sampling frequency decreases with the bit resolution M which yield to lower number of samples than for the discrete-time ADC. Certainly, the results are slightly different from an ECG to another since the number of samples depends on the input signal amplitude and frequency ranges.

To sum up, the LC-ADC sampling efficiency depends on the amplitude resolution, M, which defines the number of the reference levels, and the counter resolution, N, which must be maintained as high as possible to avoid overflowing the counter in low frequency and low amplitude regions of the ECG [32]. Moreover, in high frequency and high amplitude waves, the LC-ADC activity is increased. This fact is illustrated in Fig. 2 where 66.6% of the output samples are representative of the QRS complex for an example of 3-bit LC-ADC.

In this section, it is shown that the LC-ADC is sensitive to the values of the reference levels. Thus, in high slope regions like the QRS complex, the more the resolution of the LC-ADC amplitude is, the more the level-crossings are detected. That reduces the CR. Thus, the total number of samples can be higher than for a conventional discrete-time ADC and no compression is achieved, as for a 10-bit LC-ADC resolution.

Therefore, in this paper, LC-ADC parameters are chosen as follows: 10 mV for the full-scale, M equal to 8 bits for the resolution, N equal to 12 bits for the counter resolution and F_c equal to 10 kHz for the counter clock frequency. Besides of sampling with the LC-ADC, compression is needed to compress or to further compress LC-ADC amplitude and time intervals outputs. Since compression methods based on wavelet decomposition are commonly used in uniformly-sampled ECG compression, it is intuitive to inspect their performances in the case of continuous-time sampled data [15].

Fig. 5 shows the block diagram of a cardiac acquisition system incorporating an LC-ADC and a wavelet-based compression block for online acquisition. When appropriately designed, the LC-ADC performs compressed acquisitions of the analog signals. The wavelet transformation stage realizes discrete decompositions to

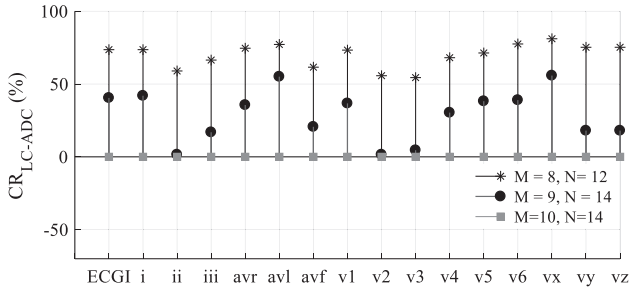

Fig. 3. LC-ADC compression ratio versus ECG leads, counter resolution and LC-ADC bit resolution.

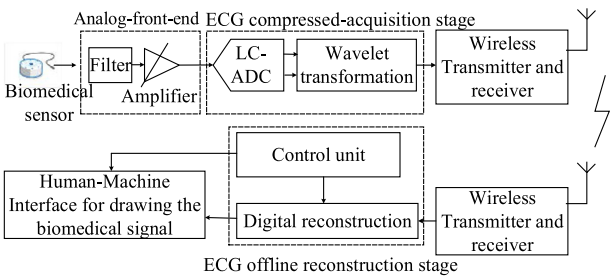

Fig. 5. Block diagram of the LC-ADC and wavelet-based acquisition system.

extract a compressed representation of the sampled data. After source encoding, radio transmission and source decoding, the digital reconstruction block performs signal decompression and linear interpolation to recover uniform samples. The control unit manages the digital reconstruction block.

In the next section, the wavelet transformation block is studied and designed regarding a circuit implementation purpose to improve the compression ratios of ECG acquisition and data compression.

3. DWT-based ECG compression methodology

In this section, a brief mathematical definition of the DWT and its relationship with sparsity are given as reported in literature. Then, the design of DWT-based decomposition stage is given according to multiresolution analysis and aiming at circuit implementation. Finally, the methodology of the compression study is presented followed by some compression parameters definitions to evaluate wavelet decomposition performances.

3.1. Discrete wavelet transform for compression

The DWT is a set of linear projections performed on a sampled signal, x, that generates a vector of discrete data, s [37]. The relation between x and its respresentation s on a given basis matrix Ψ is given in (3).

$$x = \Psi s \tag{3}$$

Thus, s, called the coefficients' vector, is a different description of x in the domain described by the wavelet or synthesis matrix Ψ. Each coefficient of s, α_i, is the scalar product of x and ψ_{Ai} as in (4), where Ψ_A is the analysis matrix or decomposition matrix which is the inverse of Ψ and ψ_{Ai} its i^{th} row.

$$\Psi^{-1}x = \Psi_A x = s \ \text{ with } \ \langle \psi_{Ai}, x \rangle = \alpha_i \tag{4}$$

In some analog and digital signal processing technique, using the computed signal s instead of x could be better as it represents the original signal x in a basis Ψ, which gives s proprieties that simplifies the processing [38]. In fact, x could be compressible regarding Ψleading to a coefficients' vector s in which the total number of significant coefficients, K, is small compared to the length, D, of s. In this case, s can be transformed in a sparse vector by keeping the largest K coefficients and setting others to zero. Besides, the coefficients α_i, especially the K largest ones, present relevant signal features that are involved in machine learning algorithms [3,6].

It directly follows from (4) that x can be approximately recovered from its sparse projections without high distortion as given in (5),

$$\widehat{x} = \sum_{u \in V} \alpha_u \psi_u, \tag{5}$$

with $V = \{i \in [\![1, D]\!] / \exists \tau \in \mathbb{R} / |\alpha_i| > \tau\}$ and $\#V = K$

where $\widehat{x}$ is the decompressed version of x when only K significant wavelets ψ_u are selected among the D available wavelets, $\#$ denotes the cardinality and τ is a threshold to decide if a coefficient is selected. If the coefficients' vector s is sparse then the number of significant coefficients, K, is very small compared to the length of s, D.

When the wavelet matrix Ψ is orthogonal, its inverse, Ψ_A, coincides with its adjugate. If the matrix involves only real values then Ψ_A is its transpose Ψ^T, and the decompression is simply done with the columns of Ψ that are the rows of Ψ_A. In this way, compared to non-orthogonal wavelets and for same compression performances, orthogonal wavelet families are advantageous with considerable reduction in computational and memory cycles needed for the algorithmic processing steps [26].

3.2. Multiresolution analysis and compression stage design

A wavelet family is created by translation and dilation of a mother wavelet, ψ_1. The obtained functions have a small number of non-zero entries compared to the length of mother wavelet support. To simplify, the orthogonal set of wavelet functions is presented in (6). They are obtained by binary dilation and dyadic translation of the mother wavelet where $\psi_{i,n}$, is the i^{th} wavelet function with a translation factor n and L is the decomposition level [37,39].

$$\begin{cases} \psi_{i,n}(t) = \frac{1}{\sqrt{2^i}} \psi_1\left(\frac{t - 2^i n}{2^i}\right) \\ 0 < i \leq L, \ n \in N \end{cases} \tag{6}$$

In multiresolution analysis, it is possible to compute multilevel decompositions. In fact, the space spanned by Ψ is defined as the orthogonal sum of subspaces. Each subspace is spanned by the orthogonal basis, $\Psi^i = \{\psi_{i,n}(t), \ n \in \mathbb{N}\}$. This basis is formed by the translated and scaled functions of the mother wavelet as described in (6) by varying the basis level i [38–39].

According to the multiresolution theory of Mallat [37], ψ_1 and each $\psi_{i,n}$ as defined in (6), can be characterized by a conjugate mirror filter as they present orthogonal basis. By this consideration, the wavelet decomposition or analysis can be implemented using a cascade of filters followed by down-sampling steps as presented in Fig. 6. The decomposition level, L, corresponds to the number of cascaded filters in the filter bank. At each decomposition level, wavelet transformation consists of dividing the signal into two parts: approximation and details. The approximation consists of selecting the slow signal variation. It uses a low-pass filter h to make the scale filtering step followed by a down-sampling by 2. In the same way, the details are obtained by selecting the fast evolution of the signal, which is most of the time composed by noise. The details are computed using a high-pass filter g to achieve the wavelet function and using a down-sampling by 2. Each decomposition level is performed on the last calculated approximation.

To recover the signal from approximation and details, DWT synthesis also using cascaded filter bank is applied using other mirror filters and performing up-sampling steps by 2. The bank filters are cascaded Ltimes as much as in the wavelet decomposition stage.

In order to construct the s sparse representation of x, coefficients with low values have to be zeroed. However, it is mandatory to keep a good signal representation to not distort the physician, namely the cardiologist, diagnosis. The easiest way to take a decision whether the coefficient has to be zeroed or not is to compare it to a threshold, τ [40]. Although it seems to be an easy way to shrink wavelet coefficients, choosing a good threshold that allows a good compression ratio with a minimum distortion is a hard task. In fact, the threshold process is the most commonly used for signal denoising. It consists of comparing the coefficient to a threshold, τ, in two manners. The first is the hard threshold rule in which only

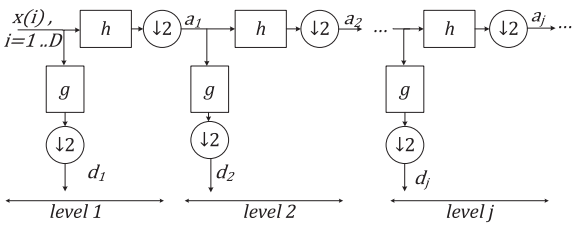

Fig. 6. DWT decomposition using cascaded filter bank where $j \leq L$.

insignificant coefficient are zeroed by applying its "keep or kill" procedure as given in (7).

$$\hat{s}(i) = \begin{cases} s(i) \ \ if \ \ |s(i)| > \tau \\ 0, otherwise \end{cases} \tag{7}$$

The second is the soft threshold rule that also consists in setting to zero all the insignificant coefficients, but it shifts other coefficients, greater than τ, by the threshold value as explained by (8).

$$\hat{s}(i) = \begin{cases} sign(s(i))(|s(i) - \tau|) & if \ |s(i)| > \tau \\ 0, \ otherwise \end{cases} \tag{8}$$

While using threshold for compression purposes, it is obvious to use the hard threshold as it keeps the most significant coefficient values.

Besides, with wavelet decomposition, the thresholding process can be either global or adaptive. This process is global when only one threshold value is computed and applied to the wavelet output regardless its level decomposition. However, if a new threshold is computed at each level of decompositon, the thresholding process is called adaptive. For sake of low complexity implementation, a global thresholding process is sought as the only threshold value, which is computed for all the decomposition levels.

Many threshold values are proposed in the literature [40–43]. In [40], the VisuShrink is proposed. It uses the hard threshold rule and is a global thresholding process with a value proportional to the standard deviation of the noise as given in (9),

$$\tau_{VisuShrink} = \sigma_{noise}\sqrt{2\log_2 D} \tag{9}$$

where σ_{noise} is the standard variation of the noise and D is the input signal length.

Although simple to be implemented, the VisuShrink threshold, also named universal threshold, has the inconvenience to reduce many coefficients which highly distort the original signal [42]. In [43], the SureShrink is introduced as an adaptive thresholding process that uses the soft threshold rule. At each level of decomposition, the SureShrink uses the minimal value between the Stein's Unbiased Risk Estimator minimum and $\tau_{VisuShrink}$ value. The goal of the SureShrink process is to minimize the mean squared error. However, it is costly to perform the Stein's estimation at each level of decomposition.

The soft-threshold is firstly introduced by Donoho in [40]. As its name suggests, it uses the soft-thresholding rule. Nevertheless, this threshold value was also used with hard thresholding rule [44–45]. It is an adaptive thresholding function whose value is given in (10) and that is not complex to compute and implement.

$$\tau_s = \sigma_{noise}\sqrt{2\log_2 D}/\sqrt{D} \tag{10}$$

Also, it is proven that the denoised signal, or as in our case the compressed signal, is as smooth as the original signal regardless the smoothness metric [45].

To sum up, for circuit implementation purposes, the ideal threshold process has to follow the hard threshold rule. It should also admit a non-complex value and ensure a smooth compressed signal to reduce the distortion. Prior to this, it is necessary to firstly select the best-fit wavelet family to implement after the LC-ADC using an iterative algorithm on Matlab. Then, a trade-off between the compression ratios of the selected wavelets, their generated distortion and their complexities has to be performed. Thus, the next subsection deals with the adopted methodology to operate Matlab simulations for wavelet family selection.

3.3. Methodology of ECG compression study and evaluation

In this paper, the compression study is done on continuous-time sampled ECG data. The tested signals are downloaded from Physionet database then sampled using the LC-ADC model. The orthogonal matching pursuit (OMP) algorithm is used to select the best-fit wavelet for compression, to compute the wavelets coefficients and to estimate the number of the K most-significant coefficients. The OMP is a predefined Matlab algorithm based on iterative application of the DWT [16]. At each iteration, the OMP computes the greatest coefficient in absolute value and provide back the signal residue that serves as input for the following iteration. Thus, this algorithm is run for K iterations that leads to the K greatest coefficients and the indexes of the most active wavelets in Ψ which are defined by the set $V = \{i \in [\![1, D]\!] / \exists \tau \in \mathbb{R} / |\alpha_i| > \tau\}$ and $\#V = K$. The recovered signal from the K most significant coefficients is compared to the original signal. Thus, the selected coefficients regarding a given signal quality can be computed. In fact, the signal quality is measured by computing the percentage root-mean square difference (PRD) [46]. It compares the ECG input signal, x, to the ECG recovered signal, $\hat{x}$, after a given processing as defined in (11).

$$PRD = \sqrt{\frac{\sum_{i=1}^{U}\left(x(i) - \hat{x}(i)\right)^2}{\sum_{i=1}^{U}\left(x(i) - \bar{x}\right)^2}} \tag{11}$$

where $x(i)$ is the i^{th} sample of x, $\hat{x}(i)$, is the i^{th} sample of $\hat{x}$, U is the number of samples and $\bar{x}$ is the mean value of x.

The defined methodology and parameters, described in this paragraph, are performed over a wide range of continuous-time sampled ECG signals covering many wavelet families. Fig. 7 shows the block diagram of the compression study to evaluate wavelet-based compressibility of LC-ADC outputs. The compression methodology is organized in 8 steps.

- The signal from Physionet database, ECG_h, is up-sampled at 1 MHz to obtain a signal with a fine time axis as with analog signals, where h varies from 1 to the total number of ECG test signals.

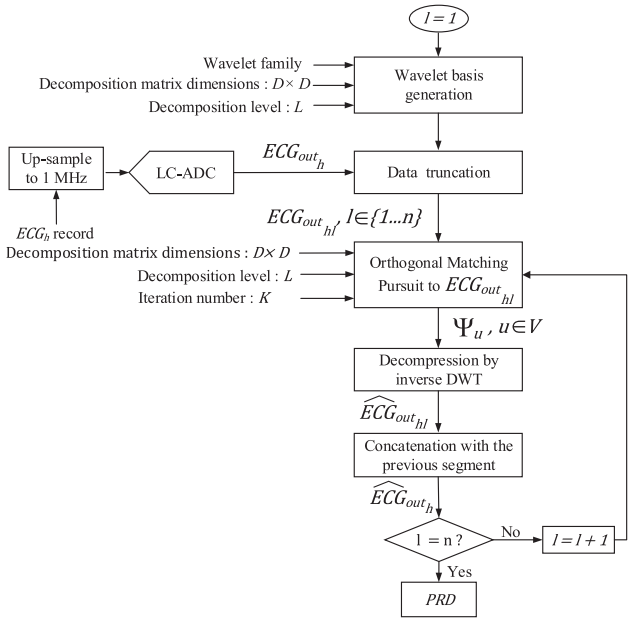

Fig. 7. Block diagram of ECG compression study.

- The up-sampled signal is converted using the LC-ADC model, which is executed in Matlab/Simulink [31].
- In order to allow the multiplication of the D-by-D basis matrix, Ψ^T, and the converted data, the output vector's length is truncated to the nearest multiple of D, $\hat{N}$, using equation (12), where $N_{original}$ and n are the original length of the digital data and the nearest multiple of D, respectively.

$$\widehat{N} = nD \text{ with } n = \lfloor \frac{N_{original}}{D} \rfloor \tag{12}$$

- The vector of length nD is split into n segments, $ECG_{out_{hl}}$ for $l = 1 \cdots n$.
- The OMP is applied separately to each segment for a fixed value of the decomposition level, L, and for the maximum number of iterations, K, which is also equal to the number of selected wavelets to represent the signal.
- In order to recover the original signal, the decomposition matrix is also applied separately to each segment using (5) for x equal to $ECG_{out_{hl}}$, to obtain $\widehat{ECG}_{out_{hl}}$.
- The decompressed $\widehat{ECG}_{out_h}$ is obtained by the concatenation of the recovered segments.
- In order to evaluate the compression in terms of decompressed signal quality for fixed values of D, K and L, the PRD, is computed as in (11) where x is the output signal of the LC-ADC, ECG_{out_h}, $\hat{x}$ is the output of the concatenation stage, $\widehat{ECG}_{out_h}$, $\bar{x}$ is the mean value of ECG_{out_h} and U is equal to $\widehat{N}$. Equation (11) is also used to measure PRD after other processing stage, where $x(i)$ is the i^{th} sample of x before a given processing, $\bar{x}$ is its mean value, $\hat{x}(i)$ is the i^{th} sample of $\hat{x}$ after the given processing and $U$is the total number of samples. In fact, in this paper, PRD is evaluated for all kinds of distortions caused by the performed ECG signal processing operations; either they are acquisition, compression, or interpolation.

In this way, the eight described steps help to extract information about PRD variations versus K for a particular wavelet family for fixed wavelet matrix dimensions, $D \times D$, and a fixed decomposition level, L. A 0-% PRD reflects a lossless compression. Otherwise, it is important to keep the PRD lower than 2% as the criterion for a very low distortion and a very good diagnosis [45]. In fact, it was demonstrated in [45] that such amount of distortion does not alter the signal and consequently not skew medical diagnosis.

Due to ECG temporal and amplitude range variation [47], the number of required wavelets to reach a 2-% PRD varies from one signal to another. Therefore, to evaluate compression efficiency of a particular wavelet family with given dimension and decomposition level regarding all the tested signals, two indicative values of K are extracted from PRD variations as in (13).

$$\begin{cases} K_{max_w} = \max\limits_{h}(K_h), \\ K_{min_w} = \min\limits_{h}(K_h), \end{cases} \quad \text{for PRD} \approx 2\% \tag{13}$$

where h varies from 1 to the total number of test signals, w varies from 1 to the total number of wavelet families, K_{max_w} and K_{min_w} are the required number of wavelets to reach a 2-% PRD for the less sparse and the sparsest ECG signal for the wavelet family, w, respectively.

Towards choosing the best wavelet family, K_{max_w} is minimized, as given in (14), where K_{opt} is used to restrict the possible choices to a smaller set of wavelet families such that only the wavelets that guarantee a 2-% PRD for all tested signals while maintaining K_{max_w} as small as possible are kept.

$$K_{opt} = \min_{w}(K_{max_w}) \tag{14}$$

Moreover, since LC-ADC outputs include amplitude and time intervals, it would be computationally interesting to use the same wavelet-decomposition conditions to reduce data volume of both time and amplitude. For this reason, sparsity of time intervals is analyzed in the tested wavelet domains using the same compression methodology as described for ECG amplitude in Fig. 7. In this way, ECG_{out_h}, $ECG_{out_{hl}}$, $\widehat{ECG}_{out_{hl}}$ and $\widehat{ECG}_{out_h}$ are replaced with TI_h, TI_{hl}, $\hat{TI}_{hl}$ and $\widehat{TI}_h$ in Fig. 7.

Finally, after choosing the best wavelet family for compression of amplitude and time intervals, PRD is evaluated for the total signal processing chain. In fact, the chain includes LC-ADC sampling, wavelet transform and finally interpolation to recover uniform ECG signal. The criterion for a good quality reconstructed ECG signal is at most 9-% PRD that maintains a good diagnostic quality [46]. In the next section, wavelet compression results of LC-ADC output amplitude based on estimated compression performances computed via OMP algorithm are presented and discussed. Then, performances are computed based on the designed compression stage which is intended to circuit implementation.

4. LC-ADC amplitude output compression

To conduct the compression study, 75 ECG test signals are downloaded. They are normal and pathologic signals selected with different shapes, amplitude ranges and pathology types from Physionet database [33]. The pathology type varies from apnea to myocardial infraction which is a challenging medical emergency. To compress LC-ADC amplitude output, all available Matlab wavelet families of the Coiflet (coif), Daubechies (db), Symlet (sym), DMeyer (dmey), biorthogonal (bior) and reverse biorthogonal (rbio) families are generated using Matlab. Simulations are operated regarding three parameters: the wavelet matrix dimensions, $D \times D$, the decomposition level, L, and the number of selected coefficients to compress the signal, K. This section begins with some preliminary results. Then, the results for the LC-ADC amplitude output best-fit wavelet are presented and discussed. Afterwards, the authors present the design of the compression stage by presenting the multiplier-free wavelet decomposition and the low-computational implementation of the thresholding process.

4.1. Preliminary simulation results

As Haar is the simplest wavelet to generate and to apply to the signals, preliminary simulations are done for many Haar wavelet matrix dimensions and decomposition levels. As explained in Section 3.2 the decomposition level corresponds to the number of cascaded filter banks in DWT implementation. In order to reduce computation and implementation complexity, the decomposition level is limited to 3. In addition, performances do not vary significantly for decomposition levels higher then 3 [10].

Besides, as wavelet matrix is invertible and matrix dimensions need to be a power of 2 to optimize the wavelet functions as in (6), the authors choose to present simulations only for D equal to 64 and 128. On the one hand, lower values may not exhibit enough wavelets with many zeros to obtain signal decompositions with small number and high values of the computed coefficients. On the other hand, higher values lead to a high-complexity hardware implementation as the parameter design D represents the memory depth of amplitude samples after the LC-ADC and before the compression stage.

PRD performances regarding the number of wavelets, K, retained by the OMP for the 75 test signals and for (L, D) equal to (2, 64), (2, 128), (3, 64) and (3, 128) are measured and plotted. However, they are not included in this paper for sake of clarity.

Thus, to lighten the plots, only the best ECG test signal case with the minimum value of K that satisfy the 2%-PRD condition, the worst ECG test signal case with the maximum value of K that satisfy the 2%-PRD condition and the middle case which corresponds to the average of the PRD regarding the 75 ECG test signals are drawn in Fig. 8. As expected, the PRD decreases when K increases. In fact, the more wavelets are discarded from their representation, the more the required information for very good quality signals is lost.

In the particular case of Haar wavelet family, with almost all ECG test signals, more than 86% of the wavelet functions are needed to reach the 2-% PRD. As shown in Fig. 8, $K_{max_{Haar}}$ is equal to 56 and 110 in the case of 64 and 128 matrix dimensions, respectively. In this case, at least 88% of Haar wavelets coefficients must not be rounded to zero to guarantee decompressed signals with 2-% PRD or less. Furthermore, $K_{min_{Haar}}$ is less than 22 and 58 in the case of 64 and 128 dimensions, respectively, which is good but guarantees a 2-% PRD only for one signal.

To sum up, preliminary simulation results show that Haar basis is not the best choice to compress the continuous-time sampled ECG signals if the 2-% PRD criterion is respected. However, using other wavelet families shows better compression results as presented in the next subsection.

4.2. Wavelet selection results

To achieve a complete study of the wavelets compression for (L, D) equal to (2, 64), (2, 128), (3, 64) or (3, 128), all available Matlab orthogonal and biorthogonal wavelets have been tested. According to Fig. 7, the OMP has been applied to compress the 75 ECG test signals after the LC-ADC sampling. The simulation results drawn in Fig. 9 considers the least value of the most significant coefficients, K, that satisfies a PRD of 2% for each signal and for each wavelet. In Fig. 9, only the extrema of the value of K are drawn among the 75 possible cases regarding the wavelet families. Thus, a variation range of K, $[K_{min_w}, K_{max_w}]$ as defined in (13), is presented for the wavelet w. For example, for the Haar wavelet and for (L, D) equal to (2,64), $K_{\min_{Haar}}$ and $K_{\max_{Haar}}$ are extracted from Fig. 8 and are equal to 22 and 56, respectively, as presented in Fig. 9 (a). It can be noticed that many wavelets are not appropriate to the compression of the continuous-time sampled ECG signals, especially the rbio3.1 wavelet. In fact, it presents the highest values of K_{max_w} and K_{min_w} for all matrix dimensions and decomposition levels. Besides, as explained in Section 3, the authors focus on the K_{max_w} rather than K_{min_w} to ensure that all the signals satisfy a PRD of at most 2% for a given wavelet. According to Fig. 9, most of the bior3.x wavelets

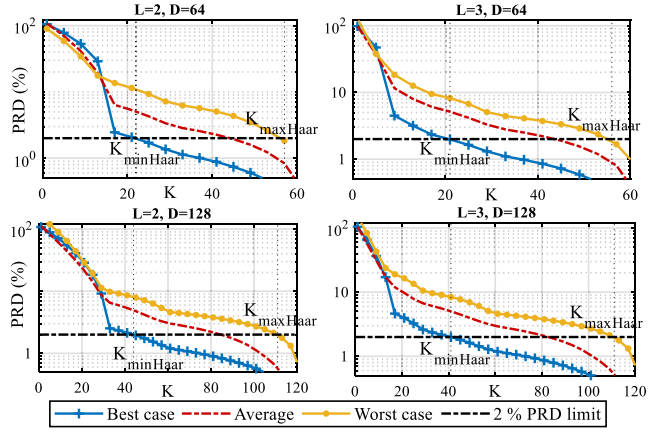

Fig. 8. PRD evolution trend for Haar wavelets versus the number of selected wavelets, K.

ensuring the optimal value of K, K_{opt} as defined in (14), are the selected ones for all L and D values.

To select the LC-ADC amplitude output best-fit wavelet, the wavelet efficiency is evaluated by the optimal samples compression ratio (SCR_{opt}) defined in (15), and the results are summarized in Table 1.

$$SCR_{opt} = \frac{D - K_{opt}}{D} \tag{15}$$

Thereby, the obtained SCR_{opt} is equal to 50% for L equal to 2 and increases to 53.12% for (L,D) equal to (3, 64) but increases only to 51.6% for (L,D) equal to (3, 128).

On the one hand, in order to keep the least computational complexity, it is mandatory to use the lowest dimensions to reduce the number of multiplications and accumulations achieved in DWT besides of reducing the depth of the samples memory. So, it is wise to keep D equal to 64 instead of 128. On the other hand, raising the decomposition level, L, increases the number of cascaded filter banks in future circuit implementation. For a sake of simplicity, and regarding the small increase of SCR_{opt} following the raise of L, the smallest value of L is retained. In this case, the optimal wavelets are the bior3.nd where nd is the decomposition filter order for L equal to2 and D equal to 64 [48].

By looking into the bior3.nd wavelet filters coefficients, it can be noticed that bior3.1 wavelet has specific coefficients allowing a multiplier-free composition and decomposition stage. Thereby, in the same perspective of reducing computational complexity, the bior3.1 is the best-fit wavelet for continuous-time sampled ECG signals. After compression, the ECG signal quality is measured thanks to the PRD metrics defined as:

- PRD_{lcadc} that measures distortion of the original signal after LC-ADC sampling and linear interpolation,
- PRD_c that measures distortion of the LC-ADC output amplitude after bior3.1 compression and its decompression,
- PRD_r that measures distortion of the original signal after LC-ADC sampling, bior3.1 compression, decompression and linear interpolation.

The simulated PRD values of ECG1, ECG2 and ECG3, in 64-dimension bior3.1 with a decomposition level L equal to 2 are summarized in Table 2. The referenced signals are respectively, the sparsest, intermediately sparse and sparseless ECG signals. It can be observed that the PRD_c is the best for the sparsest signal after lossy compression and decompression providing 0-% PRD. Besides, the PRD_r is the largest one as it combines the LC-ADC acquisition error, the compression and decompression error besides of the interpolation error. Thus, amplitude compression with 2-decomposition level 64-dimension bior3.1 guarantees an SCR_{opt} equal to 50% and final PRD values lower than 9% which reflects good signal quality.

After performing the wavelet decomposition using OMP algorithm to select the best wavelet and to estimate the number of the most significant coefficients, it is necessary to see, from a circuit implementation point of view, how to choose the 32 values to keep. Therefore, in the next paragraph, the design of the compression step through the wavelet decomposition and the thresholding process is presented and discussed.

4.3. Design of the compression stage

As presented previously, the decomposition step using bior3.1 wavelet consists of cascading filters. The coefficients of the decomposition filters, g and h, and their equivalents for the reconstruction, g_r and h_r, of bior3.1 are given in (16) [40].

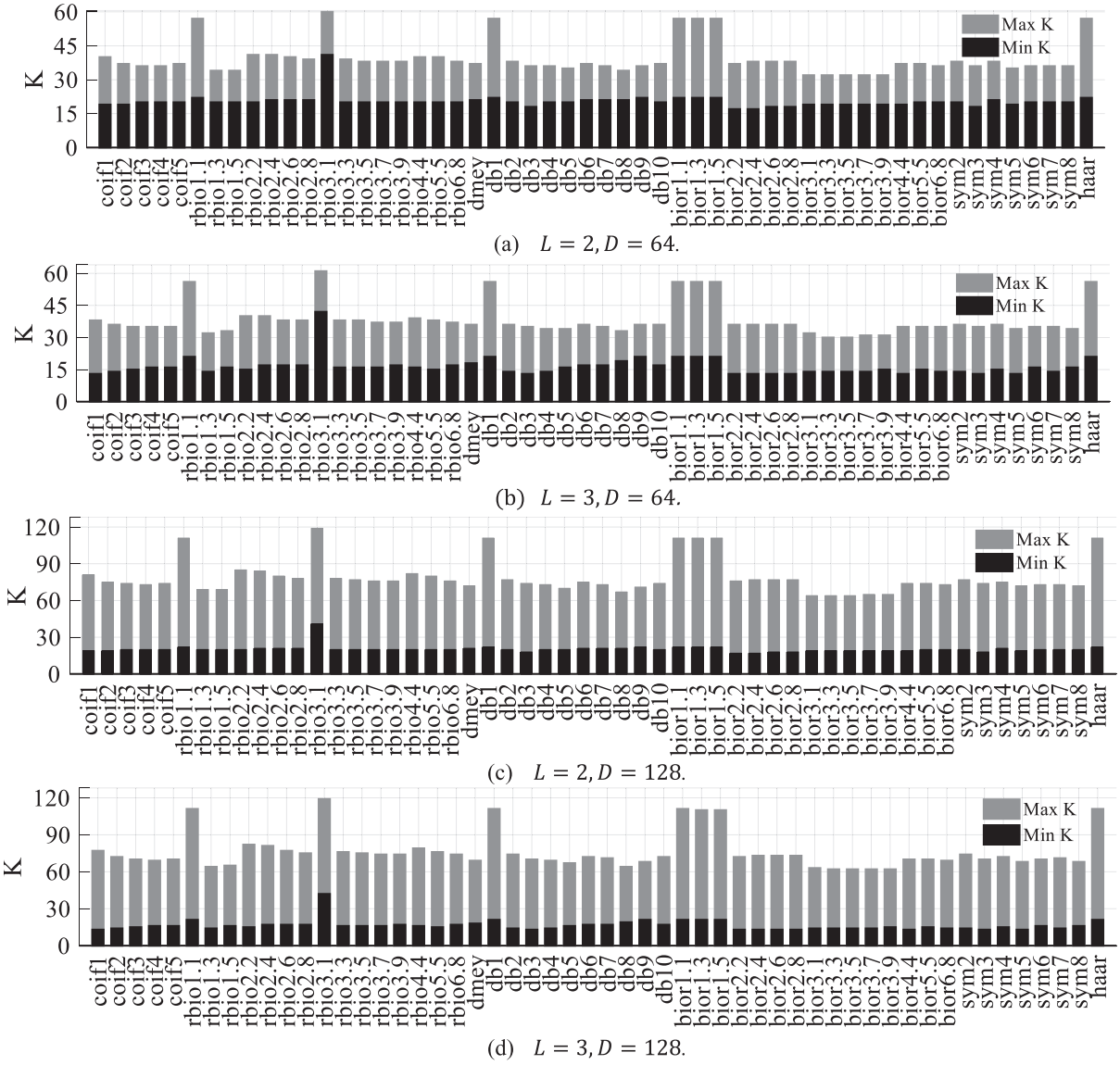

(a) $L = 2, D = 64$.

(b) $L = 3, D = 64$.

(c) $L = 2, D = 128$.

(d) $L = 3, D = 128$.

Fig. 9. Number of wavelets, K, variations vs wavelet families at different values of L and D.

Table 1
Wavelet decomposition results for a 2-% *PRD*.

(L, D)	K_{opt}	$SCR_{opt}(\%)$	Wavelet families
(2,64)	32	50	bior3.1 bior3.3 bior3.5 bior3.7 bior3.9
(3,64)	30	53.12	bior3.3 bior3.5
(2,128)	64	50	bior3.1 bior3.3 bior3.5
(3,128)	62	51.6	bior3.1 bior3.3 bior3.5

Table 2
PRD values with bior3.1 compression @ L = 2, D = 64, K = 32.

ECG test signal	$PRD_{lcadc}(\%)$	$PRD_c(\%)$	$PRD_r(\%)$
ECG1	4.19	≈ 0	4.19
ECG2	2.64	0.92	2.9
ECG3	5.12	1.86	5.34

$$\begin{aligned} h &= \sqrt{2}\left[-\tfrac{1}{4}, \tfrac{3}{4}, \tfrac{3}{4}, -\tfrac{1}{4}\right] \\ g &= \sqrt{2}\left[-\tfrac{1}{8}, \tfrac{3}{8}, -\tfrac{3}{8}, \tfrac{1}{8}\right] \\ h_r &= \sqrt{2}\left[\tfrac{1}{8}, \tfrac{3}{8}, \tfrac{3}{8}, \tfrac{1}{8}\right] \\ g_r &= \sqrt{2}\left[-\tfrac{1}{4}, -\tfrac{3}{4}, \tfrac{3}{4}, \tfrac{1}{4}\right] \end{aligned} \tag{16}$$

Being a multiple of negative exponent of 2, the decomposition consists of right shifts and additions of samples. The multiplicative factor of $\sqrt{2}$ in the decomposition, will be moved to the reconstruction side to keep using multiplier-free filters. By this way, no noise will be generated by quantizing the filter coefficients or by the addition steps. The resolution of the LC-ADC, M, is kept after all filters and decimation stages as illustrated in Fig. 6. To shrink the obtained results composed by the approximation and details, a threshold has to be applied. In fact, as estimated in the previous subsection, the threshold will reject about 32 coefficients to perform compression while keeping the 2-% PRD condition.

As the main information is kept in the approximation that is the representation of the slow variation of the signal, an obvious method to shrink the coefficients of s is to consider only this part of decomposition output and to set to zero all the details values. To validate the choice of the compression step after wavelet decomposition using the filter banks, simulation on Matlab applied to the 75 ECG signals is done. All the simulations were done using Matlab wavelet decomposition functions to simulate the filter banks. In addition, to point out results statistics, a boxplot is used. The boxplot draws the median of the data by a red line, and delimits the 25th and 75th percentile by the rectangle. This boxplot

shows the variation of the PRD for the 75 ECG signals when only approximation vector is considered. The simulation shows very high PRDs values that varies from 12 to 90% as presented in Fig. 10. This proves that some details values are as important as approximation coefficients to well recover the signal. In fact, for an input dimension $D = 64$ and a decomposition level $L = 2$, the obtained approximation vector contains only 16 values. However, as estimated in the previous subsection, $K = 32$ significant coefficients have to be kept. Thus, retaining only 16 values generates high PRD values.

Consequently, the VisuShrink is used by perfoming a hard threshold process with the thresholding value as given in (9). The standard deviation of the noise, σ_{noise}, is computed only on the noisiest signal which is the last computed details. For implementation purposes, σ_{noise} is estimated as in (17) by considering the 16 details of the second decomposition level, d_2 [43],

$$\sigma_{noise} = \frac{MAD(|d_2|)}{0.6745} \tag{17}$$

where $MAD(|d_2|)$ is the median absolute deviation of d_2 which can be also estimated, for close and positive values, to the mean of d_2. By VisuShrink threshold, PRD exceeds 0.2% and reaches 4.5% as presented by Fig. 10. This result confirms the VisuShrink disadvantage of reducing many coefficients leading to high distortions.

Therefore, the soft-threshold value, τ_s, given in (10), is then applied following the hard threshold rule, given in (7). All obtained coefficients are compared to τ_s. Fig. 10 presents the simulation results in terms of PRD and compression ratio.

Due to DWT and thresholding by τ_s, only one ECG signal returns a compression ratio of 43%. The median compression ratio is equal to 63.02%. Regarding PRD, only one signal has a PRD equal to 2.12% which is slightly higher than the PRD limit. The median value of PRD is about 0.6%. By comparing these results to values in Table 2, the 9-% PRD_r limitation will be verified as the PRD_c reaches 2.12% instead of 1.86%.

To sum up the impact of compression steps on the total compression ratio starting from sampling with the LC-ADC to DWT, the equation (2) is revised to (18) to show the effect of the samples compression ratio of the LC-ADC output amplitude, SCR_{ECG}, where SCR_{ECG} is equal to its median value 63.1%. The compression is done with the bior3.1 basis with a dimension $D = 64$, two cascaded filter bank while using the soft-threshold τ_s.

$$CR_{LCADC+DWT} = \frac{mN_{ADC} - (M \times SCR_{ECG} + N)N_{LC-ADC}}{mN_{ADC}} \tag{18}$$

The $CR_{LCADC+DWT}$ results are drawn in Fig. 11 in comparison with the LC-ADC compression ratio. By combining continuous-time sampling and compression using DWT with bior3.1 wavelets and thresholding, the achieved $CR_{LCADC+DWT}$ ranges from 65.9% to 85.8% with an increase between 4.75% and 11.4% of the CR_{LC-ADC} values.

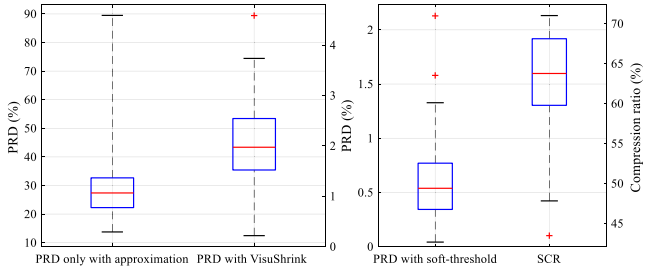

Fig. 10. (left) PRD after DWT and reconstruction with only DWT approximation coefficients and VisuShrink threshold, (right) PRD and compression ratio with threshold at τ_s.

While maintaining the PRD distortion condition as for bior3.1 family, the authors tempt to reduce implementation complexity via a multiplier-free compression stage and noncomplex thresholding process. From Fig. 12, after only bior3.1 decomposition that is intended to circuit implementation, no compression is done if no thresholding step is performed. In fact, in this case, the reconstruction algorithm allows recovering the signal with PRD approximately equal to 0%. However, if a threshold is applied, lossy compression is performed leading to a small distortion that satisfies the 2-% PRD condition. Thereby, for online compression, the authors suggest to use bior3.1 wavelet technique for its low computational complexity designs and the hard threshold rule applied globally at the τ_s value.

Besides, referring to Fig. 1, time intervals must not be ignored since the SCR_{ECG} reduces 31.5% of LC-ADC output data if only amplitude samples are compressed. Based on this observation, the authors propose to study compressibility of time intervals in bior3.1 basis in order to achieve a complete study regarding both types of LC-ADC output signals. That is the aim of the next section.

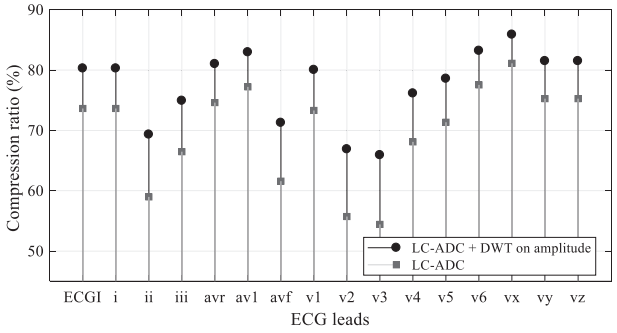

Fig. 11. CR results versus different leads of ECG signals.

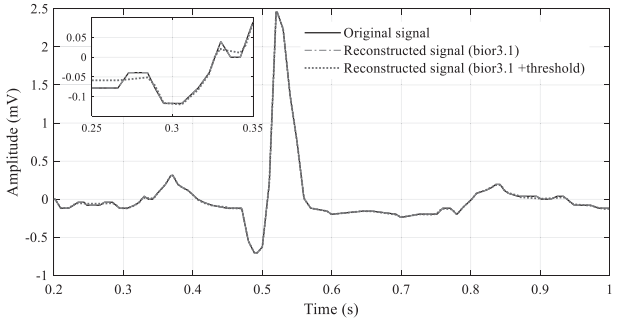

Fig. 12. Reconstructed vs original of intermediately sparse ECG signal after Bior3.1 decompostion with and without threshold.

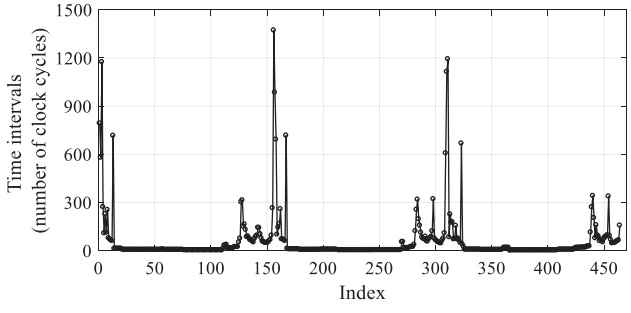

Fig. 13. Example of time intervals values.

5. LC-ADC time-interval output compression and discussion

The LC-ADC outputs are presented as a couple of data: amplitude samples and time intervals. After the compression study of the amplitude samples, it turns out interesting to test the compression algorithm on the time intervals, *TI*. Fig. 13 presents an example of time intervals values and shows few peaks while the majority of data is slightly higher than zero. This observation is encouraging to also study the compressibility of time intervals and identify a basis for which the time intervals' vector is sparse.

5.1. Wavelet selection results

As in Section 4, DWT is applied including all the available Matlab orthogonal and biorthogonal wavelets to select the best-fit wavelet and evaluate its compression performances. The range of variation of K is drawn on Fig. 14 for a basis dimension equal to 64, L equal to 2. For all simulated wavelets, K_{max_w} is almost equal to the basis dimension. Thus, no compression is observed for all ECH test signals. To point out the compression results for time intervals while varying L and D, Table 3 summarizes the values of the number of the most significant wavelets, K_{optTI}, and the samples compression ratio, SCR_{optTI}. In all the considered cases, the amount of time intervals compression is at most 11.71%. With such rates, it can be supposed that it is not worth to add computational complexity to the cardiac acquisition system.

The idea behind time compression is to use the same compression stage as in output amplitude compression. In fact, to avoid adding complexity, it was proposed to simply adjust the compression stage to reduce at most the PRD of time intervals output after decompression. Thus, the compression was supposed to be done with the bior3.1 wavelet family with $L = 2$ and $D = 64$.

However, for this configuration, the simulation on Matlab considering the 75 ECG signals shows that the bior3.1 wavelet is not selected as an optimal wavelet family to compress time intervals as presented in Table 3. Besides, according to the results in Fig. 14 and Table 3, in order to ensure a good time axis quality after decompression, 59 among 64 wavelets have to be conserved. From this study, it is estimated that almost no compression will be obtained.

Table 3
Time intervals' compression results for a 2-% *PRD*.

(L, D)	K_{optTI}	$SCR_{optTI}(\%)$	Wavelet families
(2,64)	59	7,8	rbio1.1, rbio1.3, rbio1.5, rbio2.4, rbio2.6, rbio2.8, db1, bior1.1, bior1.3, bior1.5 bior2.2, bior2.4, bior3.7, bior3.9, haar
(3,64)	58	9,37	coif5, rbio1.1, rbio1.3, db1, bior1.1, bior1.3, bior1.5, haar
(2,128)	114	10,93	bior2.8
(2,128)	113	11,71	rbio1.3, bior1.3, bior6.8

5.2. Design of the compression stage of the time intervals output

As presented in the previous section, after the bior3.1 decomposition, the threshold has to be performed. In order to reduce complexity, the threshold value τ_s has to be adjusted by an empirically computed value γ to satisfy the 2% PRD condition. Adjusting τ_s for all time intervals output signals leads to τ_{TI} as in (19). The PRD condition is also applied to time interval signals as it allows a small distortion of the signal after the reconstruction step.

$$\tau_{TI} = \gamma \sigma_{noise} \sqrt{2\log_2 D}/\sqrt{D} \tag{19}$$

Simulations with the 75 ECG signals show that in order to keep the PRD of all time interval signals less then 2%, γ must be equal to 0.1 as presented by Fig. 15.

When we apply the modified threshold τ_{TI}, the PRD reaches the value of 2.4% and exceeds the limitation value in only 3 cases among 75% of signals.

As awaited, the compression is not satisfactory as for 75% of the signals, the compression ratio is at most equal to 42%. Some signals are almost unchanged after compression at 4%-CR. The median of the time intervals SCR_{TI} is equal to 31%. To sum up the impact of the compression steps on the total compression ratio, the equation (18) is revised into (20) to show the effect of SCR_{ECG} of the LC-ADC output amplitude compression and the effect of SCR_{TI} of the time intervals compression.

$$CR_{LCADC+\mathrm{TI}} = \frac{mN_{ADC} - (M \times SCR_{ECG} + N \times SCR_{TI})N_{LC-ADC}}{mN_{ADC}} \tag{20}$$

Adding the optimal compression of the time axis improves slightly the total compression ratio as depicted in Fig. 16. The maximal increase of $CR_{LCADC+\mathrm{TI}}$ is equal to 8.4%.

In order to improve the compression ratios, the same wavelets, namely bior3.1 wavelets and the thresholding method at τ_s for

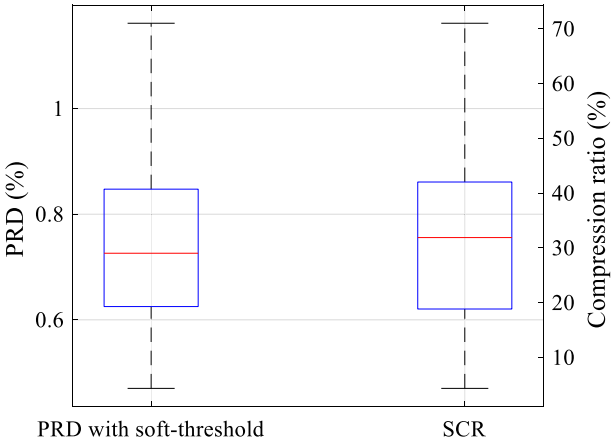

Fig. 15. Performances of the time interval signal compression.

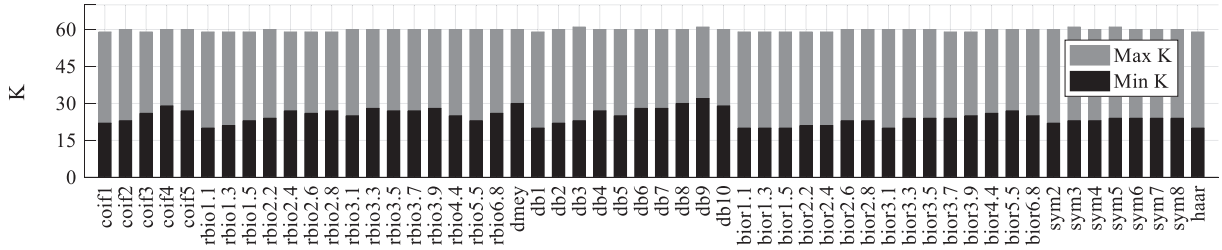

Fig. 14. Number of wavelets, K, variations vs wavelet families for L = 2 and D = 64.

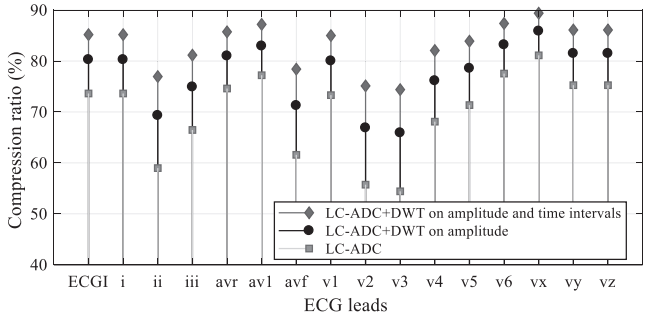

Fig. 16. CR results for LC-ADC, compressed output amplitude and compressed time intervals output using the designed compression stage versus different leads of ECG signals.

amplitude samples and τ_{TI} for time intervals values are tested. The simulation results are presented by Fig. 17 for the original signal, *ECG*1, which is the sparsest signal, and the reconstructed one after compression and decompression of both amplitude and time intervals with the designed compression stage, that are followed by linear interpolation. From Fig. 17, it is seen that a temporal offset between the original signal and the reconstructed one exists. This offset is due to the false values recovered after decompression of time intervals. In fact, since LC-ADC outputs time interval values in addition to the ECG amplitude data, the time axis has to be recovered from time interval values. Any slight error on the time intervals will be accumulated during each iteration of time axis reconstruction. Any small distortion on the time intervals leads to a large time axis distortion after 2 or 3 hearts beats. This distortion turns in a temporal offset between original and recovered signals. Besides, even if the condition of 2% PRD is satisfied, the time intervals compression leads to a highly distorted signal due to the cumulative errors on time axis. In the case of ECG1 drawn in Fig. 17, the PRD computed on the third heart beat interval sharply increases reaching 98%. This PRD will be increased for further heart beat intervals.

Clearly, referring to Fig. 17, time intervals compression with bior3.1 wavelets followed by thresholding at τ_{TI} lead to the same offset error in many signals. Thus, DWT of the time intervals seems useless. Other compression methods especially lossless ones have to be applied instead of lossy algorithms. In the next section, an overall evaluation of the proposed compression solution is discussed.

5.3. Evaluation of the proposed compression performances

The efficiency of both LC-ADC and bior3.1 decomposition followed by thresholding, is computed for a real ECG signal and compared to the conventional ADC acquisition followed by DWT and thresholding process. For instance, the aV1 signal from *s0101lrem* taken from *PTB-diagnostic* database and corresponding to myocardial infarction pathology is considered. The signal as recorded from Physionet database is sampled at 1 kHz and with the resolution of 16 bits meaning that for 1 kilo samples, 16 kilo bits are collected. In [10], an ECG compression by DWT decomposition followed by thresholding allows 68% of SCR. Such compression leads to decrease the number of bits to 5120 bits. Using LC-ADC, the 1 kilo samples will be reduced by CR_{LC-ADC} to get 227 samples of amplitude and the same number of time intervals. With the configuration of the LC-ADC, and with the proposed DWT and thresholding process only on the amplitude samples, 3398 bits are generated. This result implies a 33% of bits reduction compared to conventional ADC followed by compression using wavelet transform.

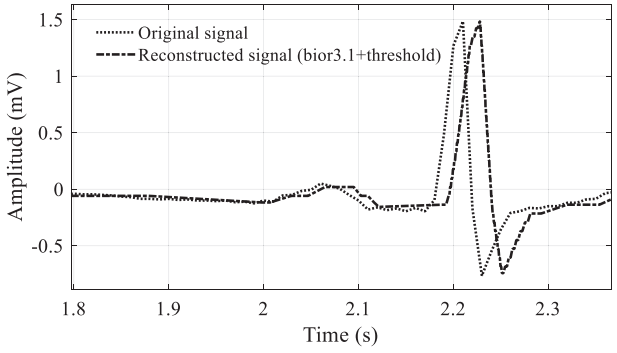

Fig. 17. Reconstructed vs original of the sparsest signal, ECG1, after filter banks-based compression of time intervals output @L = 2, D = 64 and K = 32.

6. Conclusion

In this paper, the authors suggest a study of the compressibility of continuous-time sampled ECG signals. The study is based on exhaustive simulations and comparative analysis. The study is conducted over 75 real acquisitions using 54 different wavelet families to choose the optimal wavelet for ECG compression. The design of the compression stage is proposed by choosing a multiplier-free decomposition wavelet followed by a noncomplex thresholding process. The aim of this work is the circuit implementation and the real-time process of the DWT and the threshold. As the LC-ADC delivers a couple of outputs, amplitudes and time intervals, the compression study considers both data types. Interestingly, the presented results show that amplitude compression using biorthogonal wavelets is beneficial to the continuous-time acquisition. Due to efficient digitization by the LC-ADC and then extraction of the relevant information using the DWT and the thresholding process, CRs range from 65.9% to 85.8%.

In the same perspective of reaching higher compression results, for all available Matlab wavelets, time intervals compression is evaluated and its implementation study is also proposed. It is shown that data volume is reduced at most by only 8.4%. Besides, even when distortions are slight on the reconstructed time intervals, a cumulative error in ECG reconstructed signals leads to a time shift of the decompressed signal. Therefore, the authors conclude that DWT compression method is only appropriate for amplitude compression, and a lossless compression is required for time intervals. In future works, the authors aim to nest the proposed work in an e-Health solution for heart pathology prediction and decision support system. They are involving machine learning algorithms for LC-ADC output classification based on supervised learning algorithms that admit DWT as feature extraction technique.

CRediT authorship contribution statement

Asma Maalej: Writing - original draft, Supervision, Methodology, Software. **Manel Ben-Romdhane:** Writing - review & editing, Supervision, Methodology. **Mariam Tlili:** Writing - original draft, Software. **François Rivet:** Validation, Resources. **Dominique Dallet:** Supervision, Conceptualization, Project administration. **Chiheb Rebai:** Supervision, Conceptualization, Project administration.

Declaration of Competing Interest

The authors declare that they have no known competing financial interests or personal relationships that could have appeared to influence the work reported in this paper.

Acknowledgment

This work was supported by the Comité Mixte de Coopération Universitaire Partenariat Hubert-Curien Utique [grant number (PHC-Utique) 15G1407].

References

[1] J. Dijk, B. van Loon, Scanning our past from the Netherlands: The electrocardiogram centennial: Willem Einthoven (1860–1927), Proc. IEEE 94 (12) (2006) 2182–2185.
[2] S.K. Thangavelu et al., A stand-alone EEG monitoring system for remote diagnosis, Telemed. e-Health (2016) 310–316, https://doi.org/10.1089/tmj.2015.0046.
[3] M. Nassralla et al., Patient-aware EEG-based feature and classifier selection for e-health epileptic seizure prediction, in: IEEE Global Communications Conference, 2018, pp. 1–6, https://doi.org/10.1109/GLOCOM.2018.8647660.
[4] A. Kapoor et al., Digital healthcare: The only solution for better healthcare during COVID-19 pandemic?, Indian Heart J (2020), https://doi.org/10.1016/j.ihj.2020.04.001.
[5] C.L.P. Lim et al., Deep multi-view heartwave authentication, IEEE Trans. Ind. Inf. 15 (2) (2019) 777–786.
[6] C.L.P. Lim et al., Heartrate-dependent heartwave biometric identification with thresholding-based GMM-HMM methodology, IEEE Trans. Ind. Informat. 15 (1) (2019) 45–53.
[7] V. Mondéjar-Guerra et al., Heartbeat classification fusing temporal and morphological information of ECGs via ensemble of classifiers, Biomed. Signal Process. Control 47 (2019) 41–48.
[8] B. Azmoudeh, D. Cvetkovic, Wavelets in biomedical signal processing and analysis, in: Roger Narayan (Eds.), Encyclopedia of Biomedical Engineering, Elsevier, 2019, pp. 193–212, ISBN 9780128051443.
[9] G.W. Albers et al., Heart rhythm monitoring strategies for cryptogenic stroke: 2015 Diagnostics and Monitoring Stroke Focus Group Report, J. Am. Heart Assoc. 5 (3) (2016) e002944.
[10] M. Ben-Romdhane et al. Event-driven ECG sensor in healthcare devices for data transfer optimization, Arabian J. Sci. Eng. doi: 10.1007/s13369-020-04483-w.
[11] P. Bera, R. Gupta, Hybrid encoding algorithm for real time compressed electrocardiogram acquisition, Measurement 91 (2016) 651–660.
[12] U. Satija, B. Ramkumar, M.S. Manikandan, A unified sparse signal decomposition and reconstruction framework for elimination of muscle artifacts from ECG signal, in: Acoustics, Speech and Signal Processing (ICASSP), 2016 IEEE International Conference on, 2016, pp. 779–783.
[13] H. Kim et al., ECG signal compression and classification algorithm with quad level vector for ECG holter system, IEEE Trans. Inf Technol. Biomed. 14 (1) (2010) 93–100.
[14] S. Jalaleddine et al., ECG data compression techniques-a unified approach, IEEE Trans. Biomed. Eng. 37 (4) (1990) 329–343.
[15] J. Chen, S. Itoh, T. Hashimoto, Wavelet transform based ECG data compression with desired reconstruction signal quality, Informat. Theory Stat. (1994) 84.
[16] S. Padhy, L. Sharma, S. Dandapat, Multilead ECG data compression using SVD in multiresolution domain, Biomed. Signal Process. Control 23 (2016) 10–18.
[17] C.-I. Ieong et al., A 0.45 V 147–375 nW ECG compression processor with wavelet shrinkage and adaptive temporal decimation architectures, IEEE Trans. Very Large Scale Integr. VLSI Syst. 25 (4) (2017) 1307–1319.
[18] H. Rajaguru, S. Prabhakar, E-health design with spectral analysis, linear layer neural networks and adaboost classifier for epilepsy classification from EEG Signals, Comput. Vision Bio Inspired Comput. (2018) 634–640, https://doi.org/10.1007/978-3-319-71767-8_55.
[19] R.S. Istepanian, A.A. Petrosian, Optimal zonal wavelet-based ECG data compression for a mobile telecardiology system, IEEE Trans. Inf Technol. Biomed. 4 (3) (2000) 200–211.
[20] X. Wang et al., ECG compression based on combining of EMD and wavelet transform, Electron. Lett. 52 (19) (2016) 1588–1590.
[21] G. Da Poian, R. Bernardini, R. Rinaldo, Sparse representation for fetal QRS detection in abdominal ECG recordings, in: E-Health and Bioengineering Conference (EHB), 2015, pp. 1–4.
[22] M. Elgendi, A. Mohamed, R. Ward, Efficient ECG compression and QRS detection for E-Health applications, Sci. Rep. 7 (2017).
[23] E. Allier et al., Asynchronous level crossing analog to digital converters, Measurement 37 (4) (2005) 296–309.
[24] M. Tlili et al., Level-crossing ADC modeling for wireless electrocardiogram signal acquisition system, in: I2MTC 2016, 2016. doi: 10.1109/I2MTC.2016.7520544.
[25] T. Marisa et al., Pseudo asynchronous level crossing ADC for ECG signal acquisition, IEEE Trans. Biomed. Circuits Syst. 11 (2) (2017) 267–278.
[26] M. Tlili et al., Compression study of continuous-time sampled ECG data for e-Health Applications, in: 22nd Symposium IMEKO TC 4 Symposium and 20th International Workshop on ADC Modelling and Testing (IWADC), Iasi, Romania, 2017, pp. 294–299.
[27] J.W. Mark, T.D. Todd, A nonuniform sampling approach to data compression, IEEE Trans. Commun. 29 (1) (1981) 24–32.
[28] Y. Li, D. Zhao, W. Serdijn, et al. A sub-microwatt asynchronous level-crossing adc for biomedical applications, IEEE Trans. Biomed. Circ. Syst. 7(2) (2013) 149–157.
[29] K. Kozmin, J. Johansson, J. Delsing, Level-crossing ADC performance evaluation toward ultrasound application, IEEE Trans. Circuits Syst. I Regul. Pap. 56 (8) (2009) 1708–1719.
[30] A.L. Mansano, Y. Li, S. Bagga, W.A. Serdijn, An Autonomous Wireless Sensor Node With Asynchronous ECG Monitoring in 0.18 μ m CMOS, IEEE Trans. Biomed. Circuits Syst. 10 (3) (2016) 602–611.
[31] L. Bengtsson, Single-chip implementation of level-crossing ADC for ECG sampling, J. Electr. Electron. Syst. 6 (2017) 1–6.
[32] M. Tlili et al., Level-crossing ADC design and evaluation methodology for normal and pathological electrocardiogram signals measurement, Measurement 124 (2018) 413–425.
[33] G.B. Moody, R.G. Mark, A.L. Goldberger, PhysioNet: a web-based resource for the study of physiologic signals, IEEE Eng. Med. Biol. Mag. 20 (3) (2001) 70–75.
[34] P.G. Steg et al., ESC Guidelines for the management of acute myocardial infarction in patients presenting with ST-segment elevation, Eur. Heart J. 33 (20) (2012) 2569–2619.
[35] T. Marisa et al., Bufferless compression of asynchronously sampled ECG signals in cubic Hermitian vector space, IEEE Trans. Biomed. Eng. 62 (12) (2015) 2878–2887.
[36] F.-S. Jaw, Y.-L. Tseng, J.-K. Jang, Modular design of a long-term portable recorder for physiological signals, Measurement 43 (10) (2010) 1363–1368.
[37] S. Mallat, A Wavelet Tour of Signal Processing, third ed., Academic Press, 2009, pp. 263–376, ISBN 9780123743701.
[38] I. Daubechies, Ten lectures on wavelets. SIAM, 1992.
[39] J.-M. Lina, M. Mayrand, Complex daubechies wavelets, Appl. Comput. Harmon. Anal. 2 (3) (1995) 219–229.
[40] D.L. Donoho, De-noising by soft thresholding, IEEE Trans. Inf. Theory 41 (3) (May 1995) 613–627.
[41] F.M. Bayer, A.J. Kozakevicius, R.J. Cintra, An iterative wavelet threshold for signal denoising, Signal Process. 162 (2019) 10–20. ISSN 0165-1684.
[42] R. Coifman, M.V. Wickerhauser, Wavelets and Adapted Waveform Analysis: Wavelets: Mathematics and Applications, CRC Press, Wavelets, 1994.
[43] D.L. Donoho, I.M. Johnstone, Ideal Spatial Adaptation via Wavelet Shrinkage, Biometrika 81 (3) (1994) 425–455.
[44] S.G. Nikolov, M. Wolkenstein, H. Hutter, Wavelet analysis and processing of 2-D and 3-D analytical images, in: Data Handling in Science and Technology, vol. 22, Elsevier, 2000, pp. 479-550 (Chapter 20), ISSN 0922-3487.
[45] D.L. Donoho, I.M. Johnstone, Adapting to unknown smoothness via wavelet shrinkage, J. Amer. Statist. Assoc. 90 (432) (Dec. 1995) 1200–1224.
[46] Y. Zigel, A. Cohen, A. Katz, The weighted diagnostic distortion (WDD) measure for ECG signal compression, IEEE Trans. Biomed. Eng. 47 (11) (2000) 1422–1430.
[47] L. Lu, J. Yan, C.W. de Silva, Feature selection for ECG signal processing using improved genetic algorithm and empirical mode decomposition, Measurement 94 (2016) 372–381.
[48] S.Y. Hwang, J.Y. Lee, Construction of biorthogonal wavelet vectors, Linear Algebra Appl. 434 (4) (2011) 1171–1188.